

Extracting the spectral density function of a binary composite without *a priori* assumptions

Enis Tuncer

Applied Condensed-Matter Physics, Department of Physics, University of Potsdam, D-14469 Potsdam, Germany

(Received 7 October 2004; published 12 January 2005)

The spectral representation separates the contributions of geometrical arrangement (topology) and intrinsic constituent properties in a composite. The aim of this Brief Report is to present a numerical algorithm based on the Monte Carlo integration and constrained least-squares methods to resolve the spectral density function for a given system. The numerical method is verified by testing it on the well-known Maxwell Garnett expression. Later, it is applied to a well-studied rock-and-brine system to instruct its utility. The presented method yields significant microstructural information in improving our understanding of how microstructure influences the macroscopic behavior of composites without any intricate mathematics.

DOI: 10.1103/PhysRevB.71.012101

PACS number(s): 77.22.-d, 02.70.Hm, 07.05.Kf, 05.10.Ln

Theory of mixtures and their electrical properties have attracted researchers to seek a relation between overall composite properties and intrinsic properties of the parts forming the mixture (constituents) and their spatial arrangement inside the mixture.¹ Bergman² has proposed a mathematical way for representing the effective dielectric permittivity ϵ_e of a binary mixture as a function of permittivities of its constituents, ϵ_1 and ϵ_2 , and an integral equation, which includes the geometrical contributions. It is called *the spectral density representation* (SDR). After the introduction of nondestructive measurement techniques and systems, such as electrical^{3,4} or acoustic impedance spectroscopy,⁴ the impedance of materials (either pure or composite) could be recorded for various frequencies ν . Then, the frequency could be used as a probe to obtain microstructural information with the application of the SDR.⁵⁻¹¹ This can only be achieved if (i) no influence of ν on the geometrical arrangement of phases is present,¹² and (ii) the intrinsic properties of phases are known as a function of ν . Numerical⁸⁻¹⁰ and analytical⁵⁻⁷ approaches have been proposed to resolve the spectral density function (SDF) for composites. Although numerical approaches could be preferred over the analytical ones, which are empirical expressions and are not universal, they solve a nontrivial—ill-posed—inverse problem.^{8,9} Here, we apply a recently developed numerical method¹³ to extract the SDF of a binary mixture without *a priori* assumption as in analytical solutions.⁵⁻⁷ The method is based on the Monte Carlo integration hypothesis and constrained least-squares (C-LSQ) algorithm. By using this procedure the integration constant becomes continuous rather than discrete as in regularization algorithms.^{8,9} First, the verification of the proposed method is presented by considering the Maxwell Garnett (MG) effective dielectric function.¹⁴ Later, it is applied to the dielectric data of a rock-and-brine system,¹⁵ which has been also used in Refs. 5 and 6 to test their analytical expressions.

For a binary isotropic composite system with constituent permittivities ϵ_1 and ϵ_2 , and concentrations $(1-q)$ and q , and with an effective permittivity ϵ_e , the SDR is expressed as¹⁶

$$\Delta_{e1}/\Delta_{21} - A = \int_0^1 g(x)[1 + \epsilon_1^{-1}\Delta_{21}x]^{-1}dx, \quad (1)$$

where Δ is the complex and frequency dependent scaled permittivity, $\Delta_{ab} = \epsilon_a - \epsilon_b$, and x is the spectral parameter. The constant A depends on the concentration and structure of the composite, it is related to the so-called “percolation strength”⁶ and also known as the zeroth moment.⁸ The SDF is $g(x)$, and it is sought by the presented procedure. The SDF satisfies $\int g(x)dx = q$ and $\int xg(x)dx = q(1-q)/d$,^{2,6,10} where d is the geometrical dimension of the system. In the MG approximation, shape of the inclusions n , the principle term of a depolarization tensor of a single ellipsoidal inclusion, in a particulated binary composite can also be expressed as a variable in complex permittivity of dilute and isotropic mixtures; i.e., needlelike (prolate) inclusions parallel to the field direction yield $n \ll 1/3$, unidirectional cylindrical inclusions perpendicular to the field direction yield $n = 1/2$, and oblate inclusions perpendicular to the field yield $n \approx 1$.^{17,18}

The numerical procedure is briefly as follows:¹³ first the integral in Eq. (1) is written in a summation form over some number of randomly selected and fixed x_n values, $x_n \in [0, 1]$ with n less than the total number of experimental (known) data points, Δ_{e1}/Δ_{21} and $\Delta x = 1$.

$$\Delta_{e1}/\Delta_{21} - A = \sum g_n [1 + \epsilon_1^{-1}\Delta_{21}x_n]^{-1}\Delta x. \quad (2)$$

This converts the nonlinear problem in hand to a linear one with g_n being the unknowns. Later, a C-LSQ is applied to get the corresponding g_n values:

$$\min \sum [\mathbf{\Delta} - \mathbf{K}g_n]^2 \text{ and } g_n \geq 0, \quad (3)$$

where $\mathbf{\Delta}$ is a column vector of the experimental data with the subtracted constant A , $\mathbf{\Delta} = \Delta_{e1}/\Delta_{21} - A$, and \mathbf{K} is the kernel-matrix, $\mathbf{K} = [1 + \epsilon_i^{-1}\Delta_{ji}x_n]^{-1}$. In our model, we perform many C-LSQ minimization steps with new sets of randomly selected x_n values. The g_n values obtained are recorded in each step, which later build up the spectral density distribution g .

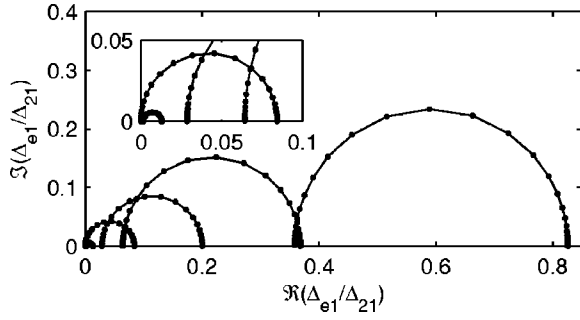


FIG. 1. Parametric plot of the scaled mixture permittivity. The symbols are the analytical model of the Maxwell Garnett equation, and the solid lines (—) are the values calculated from the spectral functions obtained from the proposed numerical method. The semicircles from large to small corresponds to $q_2 = \{0.95, 0.7, 0.5, 0.3, 0.05\}$, respectively. The inset is the enlargement of the values close to the origin for $q_2 = \{0.05, 0.30\}$.

For a large number of minimization loops, actually the x -axis becomes continuous—the Monte Carlo integration hypothesis—contrary to regularization methods.^{8,9,19} In the presented analyses below, the total number of randomly selected x values are $\sim 25\,000$. Finally, the weighted distribution of g_n versus x_n leads $g(x)$.²⁰ As a remark, Macdonald¹⁹ has explicitly shown that approaches with summation of delta functions do not suffer from the limitation of ill-posed inversion using complex-nonlinear least squares.

Application of the numerical procedure to the MG expression should yield delta sequences²² for $g(x)$.^{5,10} The dielectric function for a composite with arbitrary shaped inclusions MG composite is defined as

$$\varepsilon_e = \varepsilon_1 \{1 + dq\Delta_{21}[(1-q)\Delta_{21} + d\varepsilon_1]^{-1}\}. \quad (4)$$

The resulting SDF is then a delta function,

$$g(x) = q\delta[x - (1-q)/d]. \quad (5)$$

We choose the following values for dielectric functions of the phases: $\varepsilon_1 = 1 - i(100\varepsilon_0\omega)^{-1}$ and $\varepsilon_2 = 10 - i(\varepsilon_0\omega)^{-1}$ with $\omega = 2\pi\nu$ and $\varepsilon_0 = 8.854$ pF/m. A parametric plot of the imaginary part of Δ_{e1}/Δ_{21} against its real part is plotted for a

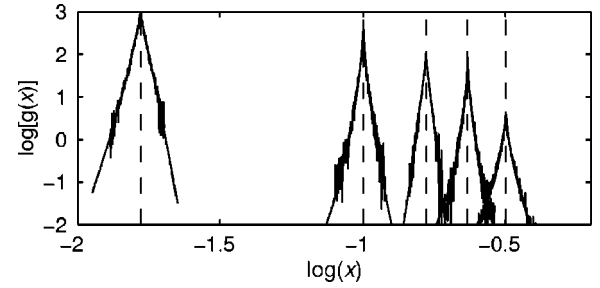


FIG. 2. Calculated spectral density distributions, which correspond to delta sequences. The distributions are presented as error bars. The spectral functions from left to right correspond to $q = \{0.95, 0.7, 0.5, 0.3, 0.05\}$, respectively. The corresponding (calculated) A values are $\{0.002, 0.012, 0.029, 0.064, 0.358\}$, respectively, for the considered concentrations. The dashed vertical lines (---) show the positions of the actual delta functions for the MG expression. The graph is in logarithmic base 10.

composite with spherical inclusions ($d=3$ and $n=1/3$) in Fig. 1. The graphs for the MG expression are semicircles. In the figure, five different concentration levels are plotted, $q = \{0.05, 0.3, 0.5, 0.7, 0.95\}$, the inset shows the enlargement close to the origin. The size and shift in $\Re(\Delta_{e1}/\Delta_{21})$ [which is A in Eq. (1)] of the semicircles are proportional to the concentration of Phase 2. The presented numerical analyses performed on the MG data yield the solid lines (—) in the figure.

The corresponding $g(x)$ are plotted as error bars in Fig. 2 on a log-log scale (logarithmic base 10). In the figure, the expected locations of $g(x)$ from Eq. (5) are also shown with dashed vertical lines (---). The $g(x)$ -distributions are analyzed by the Lévy distribution,²¹ which generates a delta sequence.²² The solid line (—) illustrate the appropriate Lévy distributions with expected values coinciding with those of Eq. (5). Various parameters from the statistical analyses and their expected values are presented in Table I. The concentration values, \bar{q} , calculated from the integration of $g(x)$ are within $<1\%$ of the expected values for the higher concentrations, and around $\sim 5\%$ for the lowest concentration. The localization parameter for x , which is the most probable value, is calculated from the integration of $xg(x)$

TABLE I. Comparison between the results of the proposed numerical approach and those of the Lévy statistics and the given analytical SDF of the MG expressions for various concentrations. The bars on the quantities indicate that they are calculated from the numerical results.

q	\bar{q}^a	\bar{x}^b	$(1-q)/d^c$	A_{in}^d	A_{out}^e	$\overline{q(1-q)}^e$	$q(1-q)^c$
0.05	0.053	0.318	0.316	0.002	0.002	0.057	0.048
0.30	0.301	0.234	0.233	0.012	0.013	0.213	0.210
0.50	0.050	0.167	0.167	0.029	0.029	0.249	0.249
0.70	0.704	0.100	0.100	0.064	0.064	0.213	0.280
0.95	0.951	0.017	0.017	0.358	0.359	0.051	0.048

^aCalculated using the resulting $g(x)$. Known from the definition of $g(x)$ —integral $\int_0^1 g(x)dx$ is equal to this value.

^bThe localization parameter for the calculated Lévy distribution. The shape parameters and the amplitude of the Lévy distributions are disregarded.

^cKnown from the definition of the SDF for the MG expression, Eq. (5). A value calculated before the numerical procedure using Eq. (1).

^dMean A value calculated during each Monte Carlo integration step in the numerical procedure, Eq. (3).

^eCalculated using the resulting $g(x)$ and x values. Known from the definition of $g(x)$ —the values is equal to the integral $\int_0^1 3xg(x)dx$.

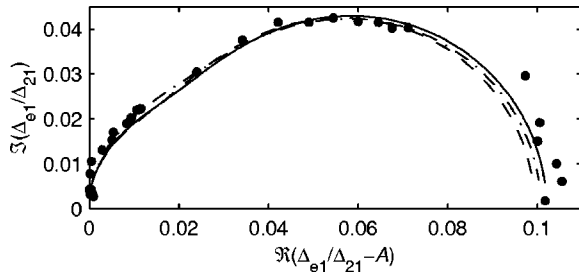


FIG. 3. Parametric plot of the scaled rock-and-brine permittivity. The symbols (\bullet) are the experimental data of Ref. 15. The chain line (- · -) is the results for the assumptions as Refs. 5 and 6, and corrected for temperature and salinity. The solid (—) and dashed (- - -) lines are results obtained by two different water and composite ohmic conductivities; $\sigma_2^0=0.85$ S/m and $\sigma_c^0=0.041$ S/m (—), and $\sigma_2^0=0.85$ S/m and $\sigma_c^0=0.038$ S/m (- - -).

and from the statistical analysis. The estimated localization parameters \bar{x} are within $<1\%$ of the actual values of the MG analytical expression.^{5,10} The product of the concentrations $q(1-q)$ or the integration of $xg(x)$ calculated have also very good agreement with those values expected from the definitions of the SDR. Observe that $\bar{x}/(1-\bar{q})$ yields the shape factor n for the spherical inclusions in the considered MG model. Finally, $A \propto q^m$ with $m=5/2$, which follows from the Archie's relation.^{5,24}

We also test our numerical procedure on a rock-and-brine composite system,¹⁵ which was studied by various scientists.^{5,6} The dielectric dispersion data had 31 points, 30 randomly selected x values were used in each Monte Carlo step, the number of Monte Carlo loops was ~ 800 . The expressions in Refs. 5 and 6 are employed to calculate the dielectric function of the brine with the ohmic conductivity of water $\sigma_2^0=0.85$ S/m. The relative permittivity of the rock is taken to be constant without any imaginary part, $\epsilon_1=7.5$. The resulting scaled dielectric quantity in Eq. (1) is presented in Fig. 3. Similar to Fig. 1, a semicircle-like shape is observed. The first analysis with the above considerations results in an unsatisfactory calculated ϵ_c as presented with the chain line (- · -) in Fig. 4. The low frequency side ($\omega < 30$ MHz) of the real permittivity has large discrepancies. The experience of the author regarding dielectric data analyses suggests that the measured values at low frequencies do not particularly satisfy the Kramers-Kronig relations.^{13,23} Consequently, application of the Kramers-Kronig relations yields lower effective composite ohmic conductivity than the original data, which was $\sigma_c^0=0.055$ S/m. Therefore two different conductivities, $\sigma_c^0=\{0.041, 0.038\}$ S/m, which result in better agreements between numerical and experimental values, are adopted.

In Fig. 5 the obtained $g(x)$ are presented with error bars. It is striking that two very distinct peaks are extracted whatever the initial considerations are for the conductivities. The $g(x)$ can be divided into three sub-SDFs, which are located around $x=\{-0, 0.004, 0.04\}$. It is clear that the original data can in a first attempt be modeled by two SDFs as delta sequences (MG expressions)^{10,11,25} without any sophisticated mathematics. However, the sub-SDF at low x values ($x < 10^{-3}$) with $g(x) \propto x^{-1}$ dependence would not be obtained

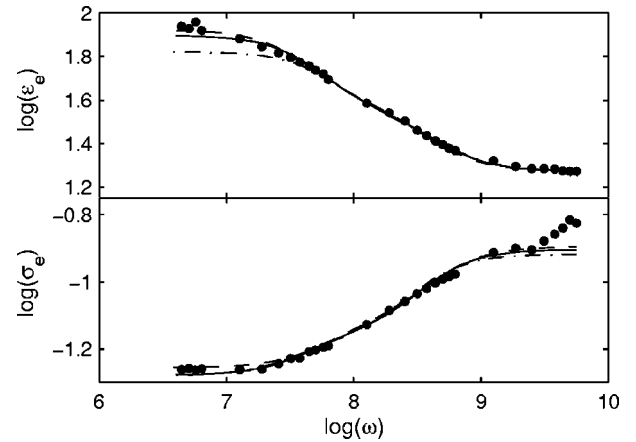


FIG. 4. Measured (\bullet symbols are the digitized data from Ref. 6) and recalculated dielectric permittivity $\Re(\epsilon_c)$ and alternating current conductivity $\sigma_c = \Im(\epsilon_c \epsilon_0 \omega)$. The chain line (- · -) is the results obtained with the same assumptions as Refs. 5 and 6 had. The line legends are the same as in Fig. 3. The graph is in logarithmic base 10.

with such an approach. The analytical SDF of Ref. 6 is displayed with the thick chain line (- · -) as a comparison. The analytical expression has been valuable to give limits for the spectral parameter x . However, in the case of Kenyon's data¹⁵ it overestimates the upper limit and could not model the sub-SDF at low x values. The two spectral parameters resolved from the sharp sub-SDF distributions at $x=\{0.004, 0.04\}$ yield concentrations $q=\{0.023, 0.111\}$ from $\int g dx = q$, respectively. The ratio $x/(1-q)$ might be used to predict the shape of pores, i.e., needlelike with $n \approx 4/23$ and spherical with $n \approx 4/11$ for the sub-SDF at $x=\{0.004, 0.04\}$, respectively. The sub-SDF situated at low x values, $g(x) \propto x^{-1}$, results in a very small concentration ($\sim 10^{-5}$), and its presence indicates that continuous percolating paths exist in the pore structure, which may involve sodium ions. The estimated zeroth moment A is 0.058, which is lower than that given by Stroud *et al.*⁵

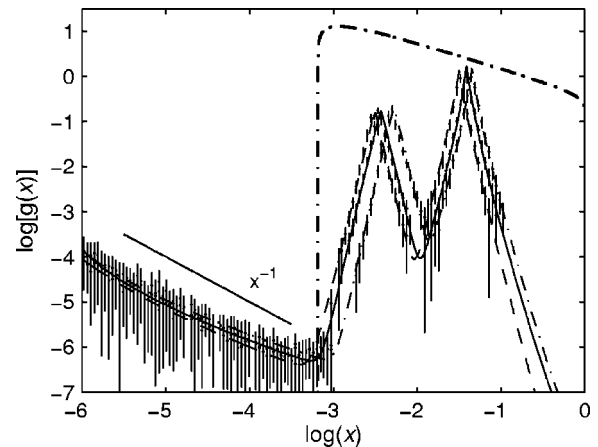


FIG. 5. Calculated spectral density distributions. The distributions are displayed as error bars. The lines represent the appropriate fitted Lévy distributions, and their legends are the same as in Fig. 3. The thick chain line is the SDF $g(x)$ of Ref. 6. The graph is in logarithmic base 10.

As a concluding remark, an effective numerical method is presented to extract the SDF of a binary composite system. It is tested on both “ideal” and measured dielectric data for composites. The proposed method not only extracts the SDF, it also yields volume fractions and effective shapes of constituents even if they are not known in advance. It is shown

that it can resolve unique SDF, which could indeed be used to obtain valuable microstructural information regarding the composite and its constituents in various research fields, in which impedance spectroscopy is used for characterization of materials, such as, polymeric, pharmaceutical, biological, building, colloidal, porous, etc.

- ¹For reviews on composites see: R. Landauer, in *Electrical Transport and Optical Properties of Inhomogeneous Media*, edited by J. C. Garland and D. B. Tanner, AIP Conf Proc. No. 40, (AIP, New York, 1978), pp. 2–43; *Progress in Electromagnetics Research*, edited by A. Priou (Elsevier, New York, 1992); S. Torquato, *Random Heterogeneous Materials: Microstructure and Macroscopic Properties* (Springer-Verlag, Berlin, 2001), Vol. 16; M. Sahimi, *Heterogeneous Materials I: Linear Transport and Optical Properties* (Springer-Verlag, Berlin, 2003), Vol. 22; G. W. Milton, *The Theory of Composites* (Cambridge University Press, Cambridge, UK, 2002); D. J. Bergman, and D. Stroud, *Solid State Phys.* **46**, 147 (1992).
- ²D. J. Bergman, *Phys. Rep.* **43**, 377 (1978); D. J. Bergman, *Phys. Rev. B* **19**, 2359 (1979); D. J. Bergman, *Ann. Phys. (San Diego)* **138**, 78 (1982).
- ³A. K. Jonscher, *Dielectric Relaxation in Solids* (Chelsea Dielectric, London, 1983); *Impedance Spectroscopy*, edited by J. R. Macdonald (Wiley, New York, 1987).
- ⁴N. G. McCrum, B. E. Read, and G. Williams, *Anelastic and Dielectric Effects in Polymeric Solids* (Wiley, London, 1967), Dover ed.
- ⁵D. Stroud, G. W. Milton, and B. R. De, *Phys. Rev. B* **34**, 5145 (1986).
- ⁶K. Ghosh and R. Fuchs, *Phys. Rev. B* **38**, 5222 (1988).
- ⁷S. Barabash and D. Stroud, *J. Phys.: Condens. Matter* **11**, 10323 (1999).
- ⁸A. R. Day, A. R. Grant, A. J. Sievers, and M. F. Thorpe, *Phys. Rev. Lett.* **84**, 1978 (2000); A. R. Day and M. F. Thorpe, *J. Phys.: Condens. Matter* **11**, 2551 (1999); A. R. Day, M. F. Thorpe, A. G. Grant, and A. J. Sievers, *Physica B* **279**, 17 (2000); A. R. Day, A. R. McGrun, D. J. Bergman, and M. F. Thorpe, *ibid.* **338**, 24 (2000).
- ⁹E. Cherkav and D. Zhang, *Physica B* **338**, 16 (2003).
- ¹⁰A. V. Goncharenko, *Phys. Rev. E* **68**, 041108 (2003); A. V. Goncharenko, V. Z. Lozovski, and E. F. Venger, *Opt. Commun.* **174**, 19 (2000).
- ¹¹Application of SDR to a biological system just using two poles is presented in J. Lei, J. T. K. Wan, K. W. Yu, and H. Sun, *Phys. Rev. E* **64**, 012903 (2001).
- ¹²The geometry should be static at each frequency, meaning that no piezoelectricity exists in the constituents, and the elastic properties of the phases should be similar otherwise there would be a nonzero displacement vector (deformation) in the composite due to the *Maxwell stress* tensor, see E. Tuncer, M. Wegener, and R. Gerhard-Multhaupt, *J. Electrostat.* **63**, 21 (2004).
- ¹³The numerical procedure to solve integral equations with the help of the Monte Carlo and C-LSQ techniques has been presented elsewhere; E. Tuncer, Lic thesis-Tech rep 338 L, Chalmers Univ. of Technol., Gothenburg, Sweden, 2000, Chap. 5, pp. 63–83; E. Tuncer and S. M. Gubański, *IEEE Trans. Dielectr. Electr. Insul.* **8**, 310 (2001); E. Tuncer, M. Furlani, and B.-E. Melander, *J. Appl. Phys.* **95**, 3131 (2004).
- ¹⁴J. C. M. Garnett, *Philos. Trans. R. Soc. London, Ser. A* **203**, 385 (1904); O. Levy and D. Stroud, *Phys. Rev. B* **56**, 8035 (1997).
- ¹⁵W. E. Kenyon, *J. Appl. Phys.* **55**, 3153 (1984).
- ¹⁶Several different notations have been used in the literature (Refs. 5, 6, and 8). Here, we rearrange the expression by Ref. 6 and obtain a similar one to those used by Refs. 5 and 8.
- ¹⁷The dielectric properties of a system with arbitrary ellipsoidal inclusions are given in R. Sillars, *J. Inst. Electr. Eng.* **80**, 378 (1937); H. Fricke, *J. Phys. Chem.* **57**, 934 (1953); W. R. Tinga, in *Dielectric Properties of Heterogeneous Materials*, Vol. 6 of *Progress in Electromagnetic Research* (Elsevier, New York, 1992), Chap. 1, pp. 1–40; P. A. M. Steeman and J. van Turnhout, in *Broadband Dielectric Spectroscopy*, edited by F. Kremer and A. Schönhalz (Springer-Verlag, Berlin, 2003), pp. 495–522; E. Tuncer and S. M. Gubański, *Doga: Turk. J. Phys.* **26**, 1 (2001). The depolarization (shape) factors for various particulated composites with ellipsoidal inclusions were calculated in these references.
- ¹⁸E. Tuncer, cond-mat/0403468.
- ¹⁹J. R. Macdonald, *J. Chem. Phys.* **102**, 6241 (1995); J. R. Macdonald, *J. Comput. Phys.* **157**, 280 (2000); *Inverse Probl.* **16**, 1561 (2000).
- ²⁰This is achieved by dividing the x axis in channels and averaging g_n in each channel.
- ²¹The expression for the Lévy statistics is $L(x; A, \bar{x}, \gamma, \zeta) = A |\exp\{t(\xi x) - (\zeta|x - \bar{x}|)^{\gamma} [1 + t\xi x / |x| \tan(\gamma\pi/2)]\}|$, where ξ , ζ , and γ are parameters that define the shape of the distribution. A and \bar{x} are the amplitude and location parameters. For details see, L. Breiman, *Probability*, Addison-Wesley Series in Statistics (Addison-Wesley, Reading, 1968); C. Walter, *Math. Comput. Modell.* **29**, 37 (1999).
- ²²E. Butkov, *Mathematical Physics*, Addison-Wesley Series in Advanced Physics (Addison-Wesley, Menlo Park, 1968).
- ²³L. Landau and E. Lifshitz, *Electrodynamics of Continuous Media*, Vol. 8 of *Course of Theoretical Physics*, 2nd ed. (Pergamon Press, New York, 1982).
- ²⁴G. E. Archie, *Trans. AIME* **146**, 54 (1942).
- ²⁵Computer simulations on “ideal” systems have illustrated that for high concentrations of inclusions or when interaction between inclusions are significant, deviations from MG expression are observed—at least two separate relaxation/depolarization processes; E. Tuncer, Y. V. Serdyuk, and S. M. Gubanski, *IEEE Trans. Dielectr. Electr. Insul.* **9**(5), 809 (2002); cond-mat/0111254; E. Tuncer, S. M. Gubański, and B. Nettelblad, *J. Appl. Phys.* **89**, 8092 (2001); **92**, 4612 (2002); J. P. Calame, *ibid.* **94**, 5945 (2003).